Available online at www.sciencedirect.com
SCIENCE DIRECT®
Journal of Power Sources 119–121 (2003) 695–700
JOURNAL OF POWER SOURCES
www.elsevier.com/locate/jpowsour

$Li_{1.01}Mn_{1.97}O_4$ surface modification by poly(3,4-ethylenedioxythiophene)

Catia Arbizzani[a], Andrea Balducci[b], Marina Mastragostino[b,*], Mauro Rossi[b], Francesca Soavi[b]

[a]*Dip. di Chimica "G. Ciamician", Università di Bologna, via Selmi 2, 40126 Bologna, Italy*
[b]*UCI-Scienze Chimiche, Radiochimiche e Metallurgiche, Università di Bologna, via San Donato 15, 40127 Bologna, Italy*

Abstract

This study reports the electrochemical characterization of non-stoichiometric $LiMn_2O_4$ spinels (commercial and home-made via the sol–gel route) covered by poly(3,4-ethylenedioxythiophene) (pEDOT) chemically grown on the oxide particle surface and of spinels without polymer covering for use in lithium-ion batteries. The results demonstrate that the pEDOT covered spinels can be suitable electrode materials without addition of conducting carbon, and that they display a slightly higher stability upon cycling than the corresponding spinels without pEDOT covering, indicating a moderate barrier effect of pEDOT which protects the inorganic particles from degradation.

Keywords: Conducting polymer; Li-ion battery; pEDOT; Non-stoichiometric spinel

1. Introduction

The spinel $LiMn_2O_4$, which has been defined as a "green" material for its non-toxicity, abundance and low-cost, has been recognized as a suitable alternative cathode to $LiCoO_2$ in lithium-ion batteries and has been the focus of growing research activities to investigate and overcome its drawback of high capacity fading, particularly at high temperature, in ethylene carbonate-dimethyl carbonate-$LiPF_6$, electrolyte, which is widely utilized in lithium-ion batteries [1–4].

Our research is focused on the development of new composite electrodes based on $LiMn_2O_4$ spinels and thiophene-based electronically conducting polymers operating at 4 V in which the polymer serves both as conducting agent and as binder and, given its electroactivity in the potential range of $LiMn_2O_4$, contributes to the composite capacity. We selected two types of $LiMn_2O_4$, one from Honeywell and the other home-made by sol–gel procedure (both can be written as $Li_{1.01}Mn_{1.97}O_4$). Non-stoichiometric spinels ensure cell parameters that prevent the Jahn-Teller effect. Several factors are recognized as responsible for the capacity fading of $LiMn_2O_4$, such as the Jahn-Teller distortion, the dissolving of manganese Mn^{2+} (Mn^{2+} arise from the disproportionation reaction of Mn^{3+} that is induced by HF present in $LiPF_6$-based electrolytes) and electrolyte decomposition. Different strategies to minimize the spinel capacity loss have been pursued, such as partial substitution of manganese cations with others and of oxygen with fluorine and by altering the surface chemistry of the spinel particles by inorganic materials [2,5,6]. The in situ polymerization of conducting polymer on $LiMn_2O_4$ is another feasible strategy because of the oxidative properties of lithium manganese oxides in an acidic medium. The growth of polypyrrole on $LiMn_2O_4$ operating at 4 V [7,8] and of pEDOT into V_2O_5 [9] has already been investigated. By pursuing this strategy, we produced and characterized a composite based on a non-stoichiometric spinel and poly(3,4-ethylenedioxythiophene) (pEDOT) operating at 4 V [10] for the first time. We found that this was the best procedure among those tested for composite electrode preparation with pEDOT because it assures good electric contact between the inorganic particulate and the organic conductor, which enables the electronic charge transfer to lithium manganese oxide.

The present paper deals with non-stoichiometric spinels covered by pEDOT chemically grown on the oxide particle surface to prevent direct contact of manganese oxide with the electrolyte. The results of galvanostatic charge/discharge cycles and impedance spectroscopy measurements on electrodes based on pEDOT-covered commercial and home-made $Li_{1.01}Mn_{1.97}O_4$ spinels, the latter prepared via the sol–gel route, are reported and compared to those of electrodes based

* Corresponding author. Tel.: +39-0512099798; fax: +39-0512099365.
E-mail address: mastrag@ciam.unibo.it (M. Mastragostino).

0378-7753/03/$ – see front matter
doi:10.1016/S0378-7753(03)00228-3

on spinels without polymer covering to investigate the efficacy of a polymer barrier to electrolyte.

2. Experimental

The $Li_{1.01}Mn_{1.97}O_4$ was prepared by sol–gel procedure after [11] starting from lithium and manganese acetates and glycolic acid as a chelating agent. The product was calcined at 750 °C for 10 h; the commercial $Li_{1.01}Mn_{1.97}O_4$, with 3.54 as the average Mn oxidation number, was provided by Honeywell GmbH. The particle size of both spinels, SG and HW, evaluated by SEM, was ca. 0.5 μm. The in situ preparation of the polymer $Li_{1.01}Mn_{1.97}O_4$/pEDOT composite was carried out as described in [10] by oxidation and subsequent polymerization of the EDOT on the $Li_{1.01}Mn_{1.97}O_4$ particles promoted by the lithium manganese oxide itself, given its oxidative property. The amount of polymer in the $Li_{1.01}Mn_{1.97}O_4$/pEDOT composite was evaluated from TGA measurements. $Li_{1.01}Mn_{1.97}O_4$ is also indicated *infra* with the simplest $LiMn_2O_4$ formula.

Different types of composite electrodes were prepared by lamination, at room temperature with a home-made roll lamination apparatus, on current collectors (Al grid covered with carbon, Al/C) of pastes prepared by mixing the components in a small amount of absolute ethanol; the electrodes were then dried at 80 °C under vacuum for several hours before use. Carbon Super P (MMM carbon) with a 40 nm particle size was used as conductive agent in conventional composite electrodes, and a mixture of carboxymethylcellulose sodium salt (Aldrich) and Teflon™ (Du Pont) was used as binder. The polymer composite electrodes with pEDOT as conductive agent were prepared (with and without binder) with sol–gel or Honeywell $Li_{1.01}Mn_{1.97}O_4$ covered with pEDOT and were indicated as SG/P and HW/P composite electrodes. The conventional composite electrodes with carbon as conducting agent were prepared both with electrosynthesized pEDOT (pEDOT electrochemical synthesis as described in [10]) and indicated as pEDOT/C composite electrodes, and with the sol–gel or commercial $Li_{1.01}Mn_{1.97}O_4$ indicated as conventional SG/C or HW/C composite electrodes. The cells were tested at 32, 55 or 75 °C (±1 °C) using conventional air thermostatic ovens. Table 1 summarizes the different electrode compositions, which are labeled with different lower case italic letters and given in w/w%. The loading of the composite electrodes was in the range 15–25 mg cm^{-2} of $LiMn_2O_4$.

The composite electrodes were assembled in dry-box as per [10] in a "T-shaped" three-electrode Teflon™ cell with Li in excess as counter electrode, Li as reference and Whatman GF/D glass separator in EC:DMC 2:1–$LiPF_6$ 1 M (Merck LP31). Charge/discharge galvanostatic cycles were performed, with cut-off potentials for the working electrode set versus Li (reference); impedance measurements were carried out in three-electrode mode with a 5 mV ac perturbation in the 100 kHz to 10 mHz range, recording 10 points/decade. The electrochemical tests were performed with a Perkin-Elmer VMP multichannel potentiostat/galvanostat, an EG&G PAR 273A potentiostat/galvanostat and an EG&G Solartron 1255 frequency response analyzer.

3. Results and discussion

The electrochemical characterization of composite electrodes started with cyclic voltammetries (CVs) in order to select the cut-off potentials of the charge/discharge galvanostatic cycles on the basis of the redox potentials of the electroactive materials. Fig. 1 shows the CVs of a polymer SG/P-*c* electrode at 0.1 mV s^{-1} and of the pEDOT/C electrode (pEDOT 80%, carbon 16.5%, binder 3.5%) at 1 mV s^{-1}. The CV of SG/P-*c* still shows the two oxidation peaks and the corresponding reduction peaks typical of the reversible two-step transformation from $LiMn_2O_4$ to λ-MnO_2. The CV of pEDOT/C indicates that we can turn the pEDOT electroactive properties to advantage in the 3.4–4.25 V range versus Li, 24 mAh g^{-1} of pEDOT being the delivered capacity of the pEDOT/C electrode in this potential range, although the pEDOT can work in a wider potential window with a capacitor-like behavior [10]. Fig. 2 reports the delivered charge cycling stability of the pEDOT/C

Table 1
Electrode compositions (w/w%), average capacity values in mAh g^{-1} of composite ($Q_{d,composite}$) and of $LiMn_2O_4$ ($Q_{d,LiMn_2O_4}$) from galvanostatic charge/discharge cycles at *C*/5 between 3.4 and 4.25 V vs. Li (reference) in EC:DMC 2:1–$LiPF_6$ 1 M of conventional and polymer composite electrodes at 32 °C

Preparation code	$LiMn_2O_4$ (%)	pEDOT (%)	C (%)	Binder (%)	$Q_{d,composite}$ (mAh g^{-1})	$Q_{d,LiMn_2O_4}$ (mAh g^{-1})
SG/P-*c*	76.2	20.3	–	3.5	90	118
SG/P-*d*	79.0	21.0	–	–	78	98
SG/C-*a*	84.7	–	8.4	6.9	98	116
SG/C-*c*	75.0	–	21.5	3.5	90	120
HW/P-*c*	75.0	21.5	–	3.5	83	110
HW/P-*d*	77.7	22.3	–	–	79	101
HW/C-*a*	84.3	–	8.3	7.4	89	106
HW/C-*b*	81.5	–	15.0	3.5	98	120
HW/C-*c*	75.0	–	21.5	3.5	99	132

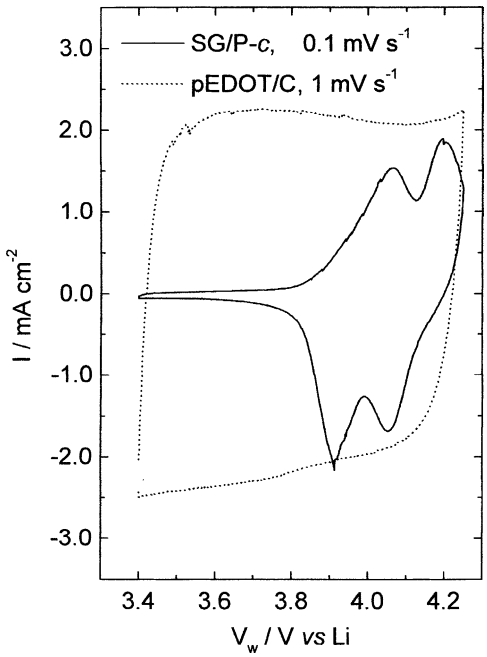

Fig. 1. CVs in EC:DMC 2:1–$LiPF_6$ 1 M of a SG/P-*c* (15.4 mg cm^{-2} $LiMn_2O_4$) at 0.1 mV s^{-1} and of a pEDOT/C (pEDOT 80%, carbon 16.5%, binder 3.5%, 19.5 mg cm^{-2} pEDOT) at 1 mV s^{-1}.

composite electrode to repeated galvanostatic charge/discharge cycles at 2.1 mA cm^{-2} between 3.4 and 4.25 V versus Li and demonstrates the high cycling stability of pEDOT/C (25 mAh g^{-1}, >99% coulombic efficiency).

To determine the optimum performance of the two selected spinels, galvanostatic charge/discharge cycles at *C*/5 between 3.4 and 4.25 V versus. Li (reference) were carried out on composite electrodes of different carbon-to-$LiMn_2O_4$ mass ratio. In addition to the electrode composition, Table 1 shows the average capacity values (average of three to four electrodes) calculated from the second cycle at *C*/5 in mAh g^{-1} of composite and of $LiMn_2O_4$. These capacity data show that while in the case of HW/C the increase of the carbon-to-$LiMn_2O_4$ ratio results in better performance of $LiMn_2O_4$, in the case of SG/C the carbon-to-$LiMn_2O_4$ mass ratio appears to influence the electrode performance less. The capacity values of polymer composite

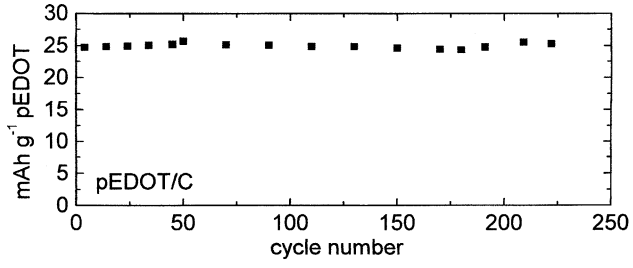

Fig. 2. Capacity at different galvanostatic charge/discharge cycles of a pEDOT/C (pEDOT 80%, carbon 16.5%, binder 3.5%, 19.5 mg cm^{-2} pEDOT) in EC:DMC 2:1–$LiPF_6$ 1 M at 2.1 mA cm^{-2} in the 3.4–4.25 V potential range.

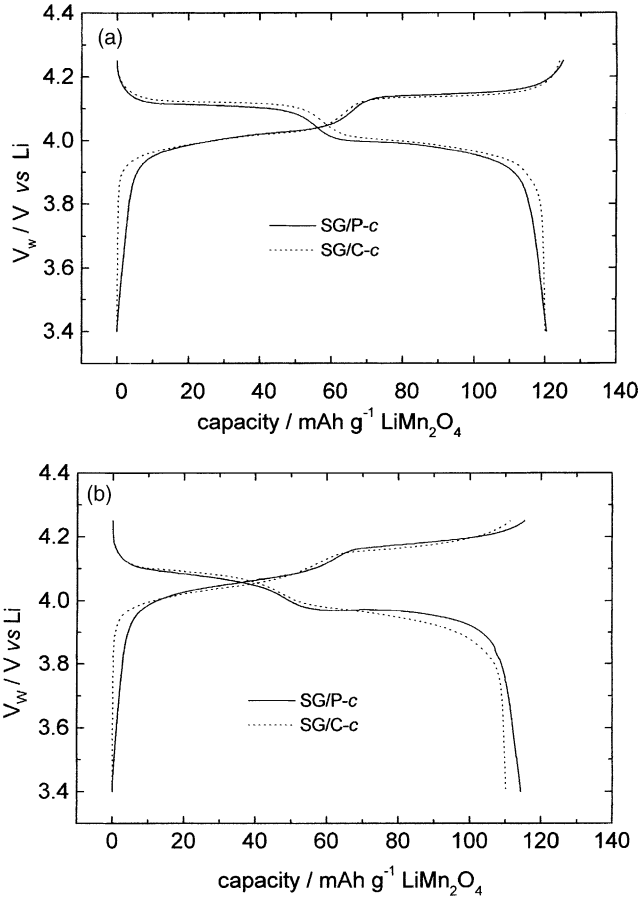

Fig. 3. Galvanostatic charge/discharge cycles of a polymer SG/P-*c* composite electrode (18.1 mg cm^{-2} $LiMn_2O_4$) and of conventional SG/C-*c* composite electrode (18.6 mg cm^{-2} $LiMn_2O_4$) (a) at 0.51 mA cm^{-2} (*C*/5, solid line) and at 0.53 mA cm^{-2} (*C*/5, dotted line), respectively; and (b) at 2.58 mA cm^{-2} (1C, solid line) and at 2.64 mA cm^{-2} (1C, dotted line), respectively.

electrodes referred to the $LiMn_2O_4$ mass are overestimated in that they also contain the pEDOT contribution of ca. 5 mAh g^{-1} of composite [10]. Table 1 also reports the data of polymer electrodes without binder additive (HW/P-*d* and SG/P-*d*), which show that pEDOT can function also as binder; however, the performance of these electrodes has to be optimized by improving the adhesion of these composites to the current collectors.

Fig. 3 shows the voltage profiles from galvanostatic charge/discharge cycles at *C*/5 and 1C of a conventional SG/C-*c* electrode and of a polymer SG/P-*c* electrode with a similar ratio between conductive additive (carbon or pEDOT) and $LiMn_2O_4$. The voltage profiles clearly show that the electroactivity of pEDOT contributes to the charge/discharge processes throughout the potential range. Indeed, the polymer SG/P-*c* electrodes, unlike the conventional SG/C-*c*, begin to be charged at potentials lower than 3.9 V versus Li and discharged at potentials lower than 3.8 V versus Li. The data indicate that pEDOT is a good conductive agent; a likely different morphology of SG and HW precursors may affect the homogeneity of the polymer's

growth in the corresponding polymer composites, which in turn reflects on the efficacy of pEDOT as conducting agent. In the case of commercial $LiMn_2O_4$ nanometric carbon assures better electric contact among $LiMn_2O_4$ particles. Because of the higher porosity of the carbon compared to that of pEDOT, a better electrolyte permeability can be envisioned in the composite cathode with carbon as conductive additive. On the other hand, a higher electrolyte permeability in the composite cathode may adversely affect the cycling stability, while in the less porous polymer composites pEDOT may act as a barrier to the electrolyte and protect $LiMn_2O_4$ from the degradation promoted by HF in EC–DMC–$LiPF_6$.

Repeated galvanostatic charge/discharge cycles at 1C at 32 and 55 °C on polymer composite electrodes were performed and, on the basis of 100 cycles, the capacity fading of these electrodes was evaluated. For comparison, the same tests were carried out on conventional composite electrodes and the results are reported in Table 2, which lists the average capacity values (average of three to four electrodes) of the initial cycles at 1C, the percentage average capacity fade throughout 100 cycles evaluated between the cycle with maximum capacity and the 100th cycle, and the working temperature. Fig. 4 compares the capacity values delivered at different cycle numbers by polymer and conventional composite electrodes based on sol–gel non-stoichiometric spinel. A certain dispersion of capacity and coulombic efficiency (see figure caption) may be ascribed to gaseous products inside the cell. The data in Table 2 and Fig. 4 indicate that pEDOT has a moderate barrier effect on $LiMn_2O_4$, which is more marked for HW/P than for SG/P.

Efforts to better understand the capacity fade phenomena of the composite electrodes during cycling were made by studying the discharge voltage profile modifications upon cycling. Lithium insertion/extraction in $LiMn_2O_4$ spinel occurs in two steps: a two-phase process around 4.1 V, in which two cubic phases coexist, and a single phase process around 3.9 V, where the cubic lattice parameter varies

Table 2
Average capacity values of composite electrodes in mAh g^{-1} of composite ($Q_{d,composite}$) and of $LiMn_2O_4$ ($Q_{d,LiMn_2O_4}$) from galvanostatic charge/discharge cycles at 1C between 3.4 and 4.25 V vs. Li (reference) in EC:DMC 2:1–$LiPF_6$ 1 M, and capacity fade over 100 cycles

Preparation code	$Q_{d,composite}$ (mAh g^{-1})	$Q_{d,LiMn_2O_4}$ (mAh g^{-1})	T (°C)	Capacity fade in 100 cycles (%)
SG/P-*c*	84	110	32	22
SG/P-*d*	55	70	32	27
SG/C-*c*	83	111	32	24
SG/C-*c*	81	108	55	38
HW/P-*c*	72	96	32	24
HW/P-*c*	71	95	55	33
HW/P-*d*	73	93	32	20
HW/C-*c*	89	119	32	32
HW/C-*c*	87	116	55	30

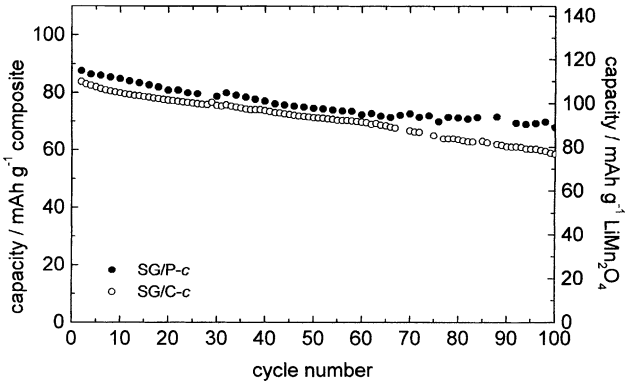

Fig. 4. Capacity at different galvanostatic charge/discharge cycles at the same C-rate 1C and 32 °C of (●) a polymer SG/P-*c* composite electrode (15.4 mg cm^{-2} $LiMn_2O_4$ at 2.20 mA cm^{-2}, $\eta = 99.6\%$, S.D. = 0.8) and of (○) a conventional SG/C-*c* composite electrode (19.4 mg cm^{-2} $LiMn_2O_4$ at 2.75 mA cm^{-2}, $\eta = 97.3\%$, S.D. =0.9).

continuously [12–14]. The capacity fade upon cycling may be due both to the dissolving of the lithium manganese oxide promoted by electrolyte decomposition products and by the losses in the charge transfer process due to the formation of inactive sites to intercalation and/or of products inhibiting the active sites. In the former case, a proportional decrease for the charge involved in the two discharge plateaus is expected. In the latter, the ratio between the charge related to the 4.1 V plateau and that related to the 3.9 V plateau should vary.

Table 3 lists for different polymer and conventional composite electrodes the capacity values for the 10th and the 100th galvanostatic discharges ($Q_{d,LiMn_2O_4}$), the stoichiometric coefficient for the total discharge process (x, calculated by taking 136 mAh g^{-1} as the theoretical capacity of the non-stoichiometric spinels), the capacities involved in the two processes at 4.1 and 3.9 V (Q' and Q''), the lithium fractions involved in the processes at 4.1 and 3.9 V (x' and x''), the differences in these parameters between the 100th and the 10th cycles and, for prompt comparison, the percentage capacity fade over 100 cycles evaluated as in Table 2. The end point of the discharge plateau at 4.1 V was evaluated by the derivative of the discharge potential profiles with respect to the involved capacity and taking the minimum of the dV/dQ_d versus Q_d curves. The data in Table 3 show that the greater capacity decrease between the 100th and the 10th cycles occurs in the 4.1 V plateau, given that $\Delta x'$ values are higher than $\Delta x''$ for all the composite electrodes. Note that the fraction of charge involved in the 3.9 V plateau is the same for all the electrodes and remains almost constant (small $\Delta x''$ values) over cycling. It thus appears that the manganese's dissolving is not the main cause of the capacity fade, given that if the manganese had dissolved, even the capacity involved in the 3.9 V plateau would have decreased proportionally. The home-made sol–gel $LiMn_2O_4$ shows improved stability with respect to commercial $LiMn_2O_4$ and the pEDOT covering has a beneficial effect on the inorganic oxide particulate,

Table 3
Average capacity values for the 10th and the 100th galvanostatic discharges ($Q_{d,LiMn_2O_4}$) at 1C and 32 °C, stoichiometric coefficient for the total discharge process (x), capacities and Li fractions involved in the processes at 4.1 and 3.9 V (Q', x', Q'' and x'), differences in Li fractions between the 100th and the 10th cycle (Δx, $\Delta x'$ and $\Delta x''$) and the capacity fade over 100 cycles

Preparation code	Cycle	Total process		4.1 V process		3.9 V process		Δx	$\Delta x'$	$\Delta x''$	Capacity fade in 100 cycles (%)
		$Q_{d,LiMn_2O_4}$ (mAh g^{-1})	x	Q' (mAh g^{-1})	x'	Q'' (mAh g^{-1})	x''				
SG/P-*c*	10	110.5	0.81	46.3	0.34	64.2	0.47	−0.15	−0.11	−0.04	22
	100	90.0	0.66	30.9	0.23	59.0	0.43				
SG/C-*c*	10	107.4	0.79	44.9	0.33	62.5	0.46	−0.17	−0.13	−0.04	24
	100	84.3	0.62	27.2	0.20	57.2	0.42				
HW/P-*c*	10	106.9	0.79	41.5	0.31	64.9	0.48	−0.17	−0.13	−0.04	24
	100	84.0	0.62	25.0	0.18	59.0	0.44				
HW/C-*c*	10	117.5	0.86	50.5	0.37	67.0	0.49	−0.29	−0.25	−0.04	32
	100	78.0	0.57	15.9	0.12	62.1	0.45				

being more evident with commercial $LiMn_2O_4$. This suggests that pEDOT may protect the oxide particles on which it has been grown, especially from the degradation products which have a detrimental effect on the sites of $LiMn_2O_4$ which are active at 4.1 V.

To further investigate the capacity fade of $LiMn_2O_4$ composite electrodes, we examined the modifications of their resistive components by impedance spectroscopy. Fig. 5 shows the impedance spectra of a polymer SG/P-*c* composite electrode after different galvanostatic cycles and at different potentials; for comparison, Fig. 6 shows the impedance spectra of a conventional SG/C-*c* composite electrode at different cycle numbers and temperatures. All the impedance spectra show a high-frequency semicircle with a maximum at a frequency of a few kHz, a medium-frequency semicircle (<10 Hz in the case of polymer composites, >10 Hz in conventional composites) and, at low frequencies, the typical behavior of a diffusion process inside the electrode materials. The high-frequency semicircle was ascribed to the charge of the external surface area of the $LiMn_2O_4$ composite electrodes, given that the corresponding capacitance values are in the order of tens of μF cm^{-2}. The related resistance was attributed to both interparticle electronic contact and ionic migration through the passivation layer and the conducting additives. This resistance has the most effect on the total electrode resistance and increases with cycle number and temperature, approaching initial values when initial temperature is restored. The reversibility of this phenomenon suggests the formation of gaseous products which are detrimental to the interparticle contact. The medium-frequency semicircle resistance was ascribed to the faradic charge process of $LiMn_2O_4$ and the parallel capacitance to the charge of the whole mass of the conducting additives—pEDOT for the polymer composites and nanometric carbon for conventional composites. For both composites the charge transfer resistance values are ca. 3–5 Ω cm^2, and for the polymer composite electrodes a capacitance value two orders of magnitude greater than that for conventional composites was estimated. The better separation between

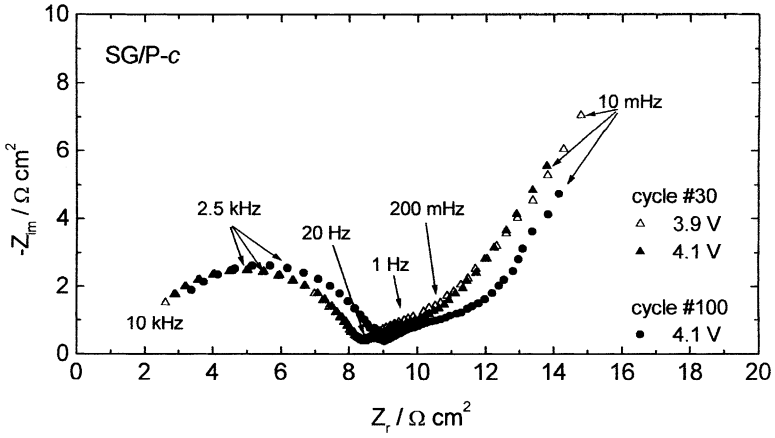

Fig. 5. Impedance spectra in three-electrode mode at 32 °C in the 10 kHz to 10 mHz frequency range of a polymer SG/P-*c* electrode recorded at 3.9 and 4.1 V vs. Li (reference) after 30 and at 4.1 V after 100 galvanostatic charge/discharge cycles at 1C in the 3.4 and 4.25 V potential range.

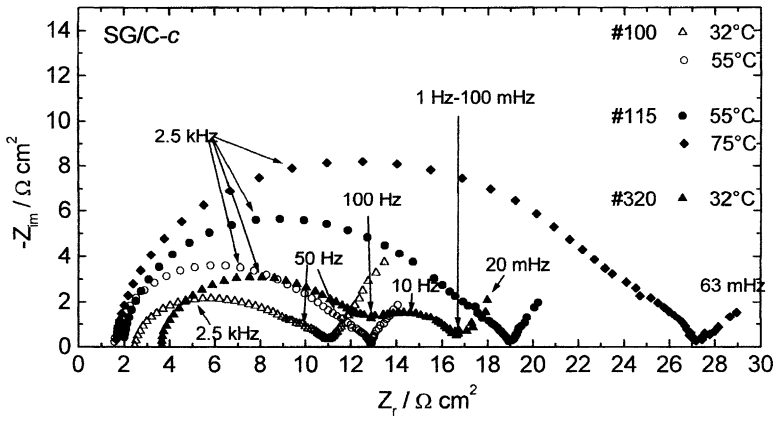

Fig. 6. Impedance spectra in three-electrode mode in the 100 kHz to 10 mHz frequency range (if not differently indicated) of a conventional SG/C-*c* electrode in the charged state at open circuit potential after different galvanostatic charge/discharge cycles at 1C in the 3.4 and 4.25 V potential range. The impedance spectra were recorded at 32 °C (△) and 55 °C (○) at the end of 100 galvanostatic cycles at 32 °C, at 55 °C (●) and 75 °C (◆) after another 15 cycles at 55 °C and at 32 °C (▲) after a further 200 cycles at 75 °C and 5 cycles at 32 °C.

the medium- and high-frequency semicircles for polymer composite electrodes than for the conventional ones is explained by the higher time constant of the medium-frequency semicircle, which is due to the higher capacitance values of the polymer composites with respect to that of conventional composites. These differences reflect those in the capacitance values of pEDOT (130 F g^{-1}) and Carbon Super P (3 F g^{-1}), which confirm the attributions we did for the semicircles. In all cases the impedance spectra evolution with cycle number shows about a 20% increase of electrode resistance, which results in a decrease of the potential range for electrode charging and, hence, in a higher capacity fade at the 4.1 V plateau. Yet, gaseous product formation which is responsible for the great resistance increase with temperature in all the systems, masks the impedance response and makes difficult the evaluation of the $LiMn_2O_4$ resistive parameters.

4. Conclusions

This work investigates the barrier effect of pEDOT on $LiMn_2O_4$ in polymer composite electrodes based on commercial and home-made non-stoichiometric spinels. The capacity fade of these polymer composite electrodes (22–24% over 100 cycles at 1C and at 32 °C) is slightly lower than that of corresponding conventional composite electrodes with nanometric carbon as conducting additive. Although the pEDOT covering has a beneficial effect on the oxide particles, its barrier effect is still insufficient to satisfy the life-cycle target of lithium-ion batteries.

The analysis of the discharge voltage profiles of all the composite electrodes indicates that their capacity fade is not due to the dissolving of Mn^{2+} induced by the electrolyte degradation products, although the latter affect the 4.1 V charge transfer process of $LiMn_2O_4$.

Further investigations on the pEDOT-covered spinels are in progress.

Acknowledgements

The authors would like to thank MURST-ENEA legge 95/95 and MURST Cofin 2000 for financial support, and Honeywell GmbH for kindly providing $Li_{1.02}Mn_2O_{4.05}$.

References

[1] J.-M. Tarascon, M. Armand, Nature 414 (2001) 359.
[2] G.G. Amatucci, N. Pereira, T. Zheng, J.-M. Tarascon, J. Electrochem. Soc. 148 (2001) A171.
[3] Y. Matsuo, R. Kostecki, F. McLarnon, J. Electrochem. Soc. 148 (2001) A687.
[4] D.D. MacNeil, T.D. Hatchard, J.R. Dahn, J. Electrochem. Soc. 148 (2001) A663.
[5] G. Amatucci, A. Du Pasquier, A. Blyr, T. Zheng, J.-M. Tarascon, Electrochim. Acta 45 (1999) 255.
[6] S.-C. Park, Y.-S. Han, Y.-S. Kang, P.S. Lee, S. Ahn, H.-M. Lee, J.-Y. Lee, J. Electrochem. Soc. 148 (2001) A680.
[7] S. Kuwabata, S. Masui, H. Yoneyama, Electrochim. Acta 44 (1999) 4593.
[8] A. Du Pasquier, F. Orsini, A.S. Gozdz, J.-M. Tarascon, J. Power Sources 81–82 (1999) 607.
[9] A. Vadivel Murugan, C.-W. Kwon, G. Campet, B.B. Kale, T. Maddanimath, K. Vijayamohanan, J. Power Sources 105 (2002) 1.
[10] (a) C. Arbizzani, M. Mastragostino, M. Rossi, Electrochem. Commun. 4 (2002) 545;
(b) C. Arbizzani, M. Mastragostino, M. Rossi, Electrochem. Commun. 5 (2003) 104.
[11] Y.-K. Sun, Solid State Ionics 100 (1997) 115.
[12] H. Huang, C.H. Chen, R.C. Perego, E.M. Kelder, L. Chen, J. Schoonman, W.J. Weydanz, D.W. Nielsen, Solid State Ionics 127 (2000) 31.
[13] M.M. Thackeray, Prog. Solid State Chem. 25 (1997) 1.
[14] T. Ohzuku, M. Kitagawa, T. Hirai, J. Electrochem. Soc. 137 (1990) 769.